

RESEARCH

Open Access



Safety and feasibility of a smart assistive bone-cement injection system: a cadaveric study

Chen Jin^{1,2†}, Ming-Liang Ning^{3†}, Rui-Jun Xu^{1,2}, Xiao-Jian Ye^{1,2}, Hao-Jie Chen^{1,2*} and Jiang-Ming Yu^{1,2*}

Abstract

Background Percutaneous vertebral augmentation is an effective and commonly surgical treatment for osteoporotic vertebral compression fractures, but the problem of bone cement leakage still cannot be prevented. It has been reported that cement leakage occurs in approximately 20% of vertebroplasty procedures, with symptomatic manifestations reported in 1.6% of cases. Leakage of bone cement into the spinal canal increases the risk for spinal cord compression and nerve injury. The objective of this study was to introduce a smart assistive device specifically designed to facilitate both cement injection control and operator protection.

Methods Two freshly frozen human cadaver specimens were used. The 2 cadaver specimens were divided according to injection method: manual (10 vertebrae, T8–L5); and motorized (10 vertebrae, T8–L5). Fluoroscopy time, cement time, volume injected, and cement distribution were recorded. Postoperative radiography and CT images were used to assess cement distribution in this cadaveric study.

Results The number of times intraoperative X-ray fluoroscopy was used for the manual injection group (6.7 ± 1.5) was significantly greater ($P < 0.001$) than that for the motorized injection group (4.1 ± 0.9). Mean cement time for the manual injection group (164.3 ± 18.7 s) was significantly greater ($P < 0.001$) than that for the motorized injection group (72.0 ± 7.2 s). There were no significant differences in the amount of cement injected in the manual vs. motorized injection group (5.2 ± 1.3 mL vs. 5.3 ± 1.0 mL; $P = 0.878$). Moreover, we found that leakage of cement outside the vertebral body was noted in 4 of 10 injected vertebrae (40%) in the manual injection group, whereas there was no bone cement leakage in the motorized injection group.

Conclusions The system exhibited more precise control of the bone cement injection dosage and better cement distribution compared with traditional manual injection. In addition, the device provided remote activation, reducing the X-ray intake of the surgeon.

[†]Chen Jin and Ming-liang Ning contributed equally to this work.

*Correspondence:

Hao-Jie Chen
chenhaojie97@126.com
Jiang-Ming Yu
yjm_st@163.com

Full list of author information is available at the end of the article



Keywords Biomedical equipment, Smart assistive, Remote handling, Percutaneous vertebral augmentation, Cadaveric trial

Introduction

Osteoporotic vertebral compression fracture (OVCF) poses a significant risk and is a major cause of disability and mortality among affected elderly individuals [1–6]. Percutaneous vertebral augmentation (PVA), including vertebroplasty and kyphoplasty, is an established procedure for treating OVCF due to its minimally invasive nature, capacity to restore vertebral height, ability to relieve pain, and ability to facilitate earlier ambulation [7, 8].

Despite their advantages, PVA procedures have notable drawbacks, the first of which is the leakage of bone cement, which can be attributed to the inherent properties of the polymers used. Among the various orthopedic cements available, acrylic bone cements based on poly (methyl methacrylate [PMMA]) are the most commonly used. At the beginning of the procedure, the cement must possess sufficient fluid consistency to facilitate manual injection, which increases the risk for leakage outside the vertebral body. Cement leakage occurs in approximately 20% of vertebroplasty procedures, with symptomatic manifestations reported in 1.6% of cases [9]. Leakage of bone cement into the spinal canal increases the risk for spinal cord compression and nerve injury [10]. Furthermore, leakage of bone cement into the paravertebral veins may result in pulmonary or cerebral embolism, and potentially fatal outcomes [10]. Another drawback is the rapid hardening of the cement at the end of the application phase, which limits the injection time to approximately 10–20 min, depending on the cement and the temperature of the operating room. The intervention must be concluded and the needles removed before this abrupt hardening. The final drawback is the need for X-ray imaging to monitor the spread of cement inside the vertebral body. This leads to continuous surgeon and patient exposure to radiation [11], which is only partially limited by uncomfortable, lead-lined clothes.

To date, little attention has been devoted to bone cement-assisted injections. In a pioneering study, Loeffel et al. [12] presented a computer-assisted injection device that coupled high-pressure cement delivery with parameter control, provided remote activation, and relied on traditional syringes as material containers for low-cost operation(s). The StabiliT system (Merit Medical Systems Inc., South Jordan, UT, USA [13]) offers a solution to polymerize bone cement in situ using radiofrequencies; however, the practitioner does not receive any feedback. These 2 strategies, in part, prompted the present study, contributing to the development of a new method to

perform both teleoperation with pressure feedback and PMMA injection management.

PVA involves X-ray-guided trocar positioning, followed by fluoroscopy-controlled cement injection. The positioning and insertion of trocars are tasks well mastered by experienced practitioners. Therefore, assistance with PVA should first focus on cement injection. The aim of this study was to introduce a smart assistive device specifically designed to facilitate both cement injection control and operator protection. Because human trials are yet to be authorized, we conducted a cadaveric study to explore the safety and feasibility of smart injection systems. Results of this study provide valuable insights into the role of “smart assistance” in PVA surgery and further clinical validation.

Materials and methods

Specimens

Two freshly frozen human cadaver specimens were used in this study, both of which underwent thorough visual inspection to ensure the absence of fractures, deformities, previous surgery, and severe spondylosis. Computed tomography (CT) was performed on the 2 specimens to assess bone quality and obtain measurements for planning the ideal puncture path. Body length (BL), width (BW), and height (BH) were separately collected from axial and sagittal CT images. The present study was granted approval by the Medical Ethics Committee of Tongren Hospital affiliated to Shanghai Jiaotong University School of Medicine, and the experimental investigation involving cadavers adhered to the ethical standards outlined in the 1964 Declaration of Helsinki. The specimens were stored at -20 °C and were thawed at room temperature for approximately 24 h prior to dissection.

Surgical technique and constructs

The 2 cadaver specimens were divided according to injection method: manual (10 vertebrae, T8–L5); and motorized (10 vertebrae, T8–L5). The cadaveric specimens were positioned prone on a surgical table. The surgical procedure involved the use of a motorized bone-cement injection system. The equipment necessary for the device included a host, bone-cement injector, powered motor, pressure pump, hydraulic valve, sterile container, pressure transducer, and controller (Fig. 1).

Manual injection specimen

The T8–L5 vertebrae were located under C-arm fluoroscopic guidance. A puncture needle was inserted into the vertebral body via the bilateral pedicle under the

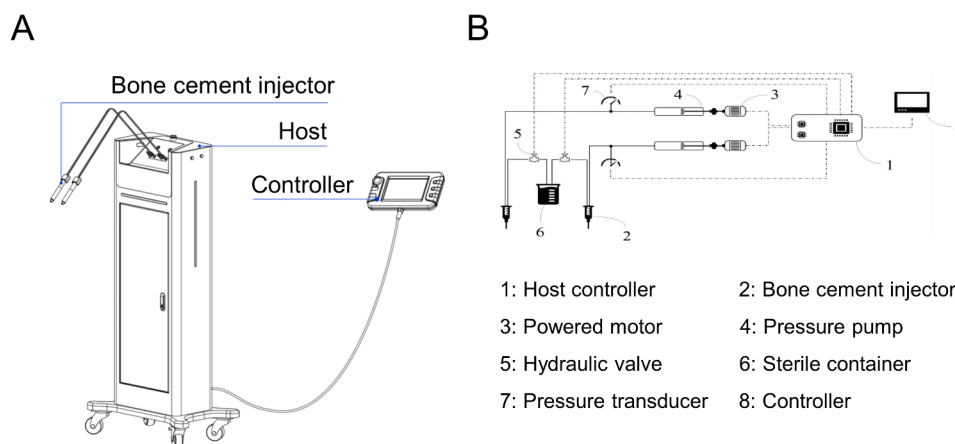


Fig. 1 Schematic of the smart assistive bone-cement injection system. (A) Overall view of the bone-cement injection device. (B) Injection device components: Host controller, bone cement injector, powered motor, pressure pump, hydraulic valve, sterile container, pressure transducer, and controller

supervision of a senior surgeon. When the working channel was set up, a low-viscosity cement (i.e., PMMA) was injected cautiously under C-arm fluoroscopy to prevent as little cement leakage as possible. Cement injection and leakage were monitored using C-arm fluoroscopy during the surgery. Approximately 30–50% of the vertebral body was filled with bone cement. The injection had to be completed and the needle had to be removed before the bone cement hardened completely. Detailed puncture techniques were important—but not the major concern—in this study. To validate adequate and uniform filling of the vertebral body, a final radiographic imaging step was performed.

Motorized injection specimen

The T8–L5 vertebrae were located under C-arm fluoroscopic guidance. The puncture needle was inserted into the vertebral body via the bilateral pedicles by the same surgeon. The PMMA cement was injected into the bone cement injector. The spatial separation of the controller from the injection device, which was directly attached to the host through a flexible connection hose, enabled remote activation from external radiation fields generated by intraoperative imaging devices. The bone cement was injected using a hydraulic injection apparatus driven by a syringe pump. Radiation exposure was low when the practitioner was positioned away from the imaging device due to the long length of the connecting hose. The surgeon manually set the required parameters (i.e., injection speed and time, unilateral or bilateral injection, and continuous or interrupted injection) using a control panel located behind a lead plate. The minimum injection speed was 0.1 mL/s. The working channel was withdrawn after the cement had hardened. During the injection, fluoroscopy enabled monitoring of bone cement diffusion inside the vertebral body. The surgical procedure is illustrated in Fig. 2.

Evaluation method

Demographic information regarding the cadaveric specimens, including age, body mass index, sex, and race, are summarized in Table 1. The present study focused on cement distribution; as such, many other variables were not analyzed. Fluoroscopy time, cement time, volume injected, and cement distribution were recorded to assess the safety and feasibility of the smart injection system after surgery. Cement time refers to the interval from the beginning of bone-cement mixing to immediately before injection. Postoperative radiography and CT images were used to assess cement distribution in this cadaveric study involving 10 thoracic and 10 lumbar vertebrae. To ensure unbiased evaluation, all assessments were independently conducted by a blinded spine surgeon.

Statistical analysis

All statistical analysis was performed using SPSS software version 19.0 (SPSS Inc, Chicago, IL, USA). If a continuous variable followed a normal distribution, it was expressed as the mean \pm standard deviation (SD), and the independent-sample *t*-test was used for the comparative analysis. A *P*-value of less than 0.05 was considered statistically significant.

Results

At the time of death, the age and BMI of specimens 1 and 2 were 75 and 77 years, and 22.2 kg/m² and 21.5 kg/m², respectively. Both the cadavers were Asian men with no history of preoperative spinal surgery or bone abnormalities (Table 1).

In this study, 20 vertebrae (T8 to L5) from each cadaver, were analyzed. The BL, BW, and BH of the T8–L5 vertebral level for the included specimens in each group are summarized in Tables 2 and 3. There were no significant differences in anatomical parameters between specimens 1 and 2 (mean [\pm SD] BL, 28.4 \pm 2.3 mm versus [vs.]

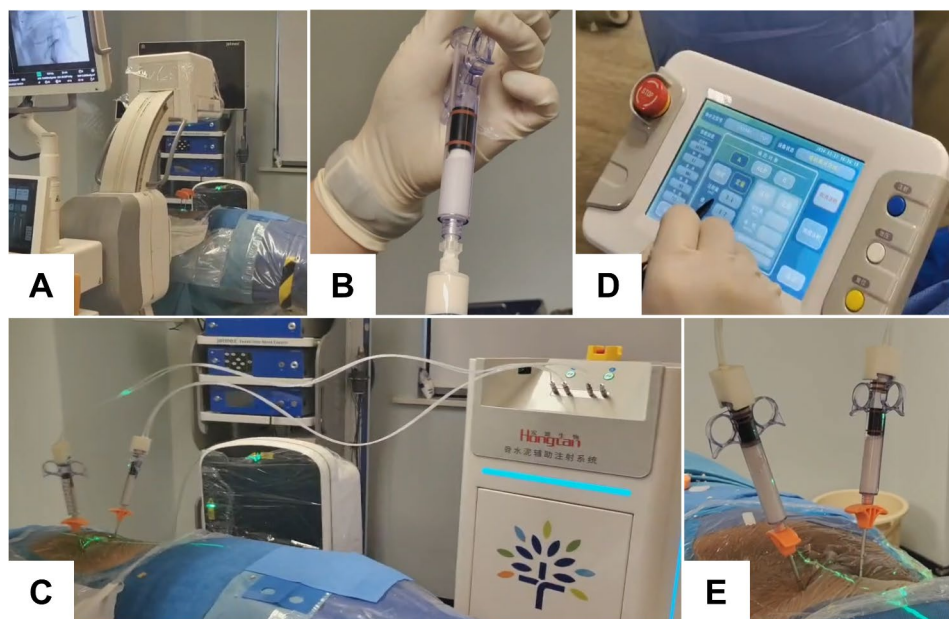


Fig. 2 Procedures of smart assistive bone-cement injection. (A) Preoperative X-ray-based planning of needle trajectory. (B) Bone cement preparation. (C) Attachment of the injector and the host through the flexible connection hose. (D) Parameter settings. (E) Bone cement injection

Table 1 Demographics of 2 cadaveric specimens

Characteristic	Specimen 1	Specimen 2
Age (years)	75	77
Body mass index (kg/m ²)	22.2	21.5
Sex	Male	Male
Race	Asian	Asian

30.3 ± 2.3 mm [*P* = 0.081]; mean BW, 35.4 ± 6.0 mm vs. 34.9 ± 5.1 mm [*P* = 0.866]; mean BH, 20.2 ± 2.5 mm vs. 20.2 ± 2.1 mm [*P* = 0.968]).

Intraoperative indicators revealed significant differences in fluoroscopy and cement times between the manual and motorized injection groups (Tables 2 and 3). The number of scopes for the manual injection group (6.7 ± 1.5) was significantly greater (*P* < 0.001) than that for the motorized injection group (4.1 ± 0.9). Mean cement time for the manual injection group

(164.3 ± 18.7 s) was significantly greater (*P* < 0.001) than that for the motorized injection group (72.0 ± 7.2 s). There were no significant differences in the amount of cement injected in the manual vs. motorized injection group (5.2 ± 1.3 mL vs. 5.3 ± 1.0 mL; *P* = 0.878).

There was a significant difference in the distribution of the bone cement between the 2 groups (Fig. 3). Immediate postoperative anteroposterior and lateral radiographs revealed that the distribution of bone cement tended to be diffuse or block type in the motorized injection group. In the manual injection group, the distribution of bone cement tended to be a double- or single-band. Postoperative axial computed tomography scans indicated that the bone cement was evenly distributed through the anterior and middle parts of each vertebral body in the motorized injection group and an uneven density distribution was found in the manual injection group. Moreover, the

Table 2 Anatomic characteristics of specimen 1 and primary data evaluation of manual bone cement injection

	BL (mm)	BW (mm)	BH (mm)	Fluoroscopy times	Cement time (s)	Cement (mL)	Cement leakage
T8	25.69	27.74	16.15	7	185	3.9	No
T9	26.11	28.42	16.84	8	165	4.6	No
T10	26.80	30.25	18.43	5	146	3.7	Yes
T11	27.05	31.20	19.20	6	140	4.5	No
T12	28.78	33.88	19.38	8	178	3.8	No
L1	27.21	36.94	23.17	9	188	6.3	Yes
L2	28.93	37.98	22.53	6	180	6.0	No
L3	29.66	39.39	21.65	7	168	6.2	Yes
L4	31.05	43.21	22.21	4	138	6.6	Yes
L5	32.78	44.61	22.41	7	155	6.8	No

BL: body length; BW: body width; BH: body height

Table 3 Anatomic characteristics of specimen 2 and primary data evaluation of smart assisted bone cement injection

	BL (mm)	BW (mm)	BH (mm)	Fluoroscopy times	Cement time (s)	Cement (mL)	Cement leakage
T8	27.13	27.50	15.83	3	68	4.3	No
T9	27.13	27.88	17.92	3	65	4.3	No
T10	28.23	32.64	19.21	4	77	4.5	No
T11	30.07	33.00	19.69	5	85	4.4	No
T12	30.74	34.43	19.74	4	70	4.3	No
L1	29.72	36.53	22.43	3	62	5.8	No
L2	32.49	36.32	22.32	4	66	6.2	No
L3	33.10	36.31	21.05	5	72	6.5	No
L4	31.19	41.00	21.34	5	80	6.3	No
L5	32.99	43.75	22.02	5	75	6.6	No

BL: body length; BW: body width; BH: body height

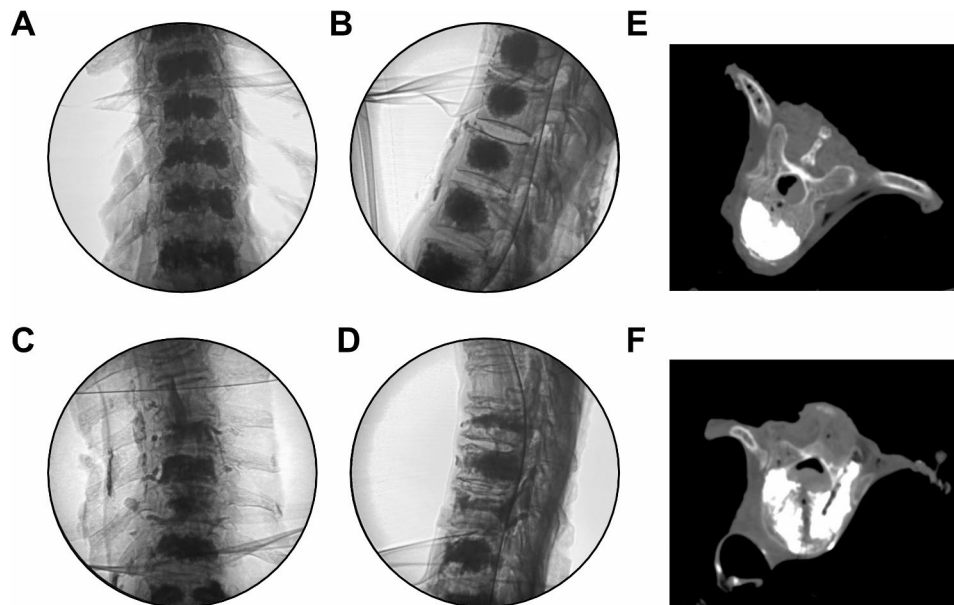


Fig. 3 Radiographic assessment of bone cement distribution. (A) Immediate postoperative C-arm anteroposterior image of bone cement distribution in the motorized injection group. (B) Immediate postoperative C-arm lateral image of bone cement distribution in the motorized injection group. (C) Immediate postoperative C-arm anteroposterior image of bone cement distribution in the manual injection group. (D) Immediate postoperative C-arm lateral image of bone cement distribution in the manual injection group. (E) Postoperative axial CT scans of bone cement distribution in the motorized injection group. (F) Postoperative axial CT scans of bone cement distribution in the manual injection group

results demonstrated that leakage of cement outside the vertebral body was noted in 4 of 10 injected vertebrae (40%) in the manual injection group, whereas there was no bone cement leakage in the motorized injection group (Tables 2 and 3). Notably, the vertebral body reached completely transpedicularly in both methods, and 4 leakage cases seen in the manual method (T10-L1-L3-L4) were not due to the wrong anatomical approach.

Discussion

PVA is widely used for OVCFs due to its simplicity and efficacy [14, 15]. Cement can intensify the fractured vertebral body and quickly relieve its symptoms [16, 17]. However, PVA is affected by many factors such as the amount of injected cement and the cement distribution pattern [18, 19]. To overcome the shortcomings

of currently used injection devices, the present study describes the use of a smart assistive bone-cement injection system for PVA. The application of this system can improve the precision control of bone cement injection dosage and better cement distribution. In addition, the device couples high-pressure cement delivery with parameter control and provides remote activation, reducing the X-ray intake of the surgeon. Therefore, our smart assistive system has potential clinical popularization and application value.

Most commercial systems for bone-cement injection are operated manually. They include a syringe whose piston is pushed either by hand, such as the Vertecem II system (DePuy Synthes, Raynham, MA, USA [20]), or via a force amplification mechanism, as the Precision Cement Delivery System (Stryker, Kalamazoo, MI, USA [21]) or

Cemento MP (Optimed, Ettlingen, Germany [22]) that both use a screw-nut system. Some manufacturers have proposed injection devices that enable an increase in the distance between the practitioner and X-ray source. The Confidence Spinal Cement System (DePuy Synthes [20]) and the Osseoflex device (Merit Medical [23]) perform such remote injections with hydraulic transmission lines (0.5–1.5 m long). However, such transmissions add uncertainty and latency, resulting in a lack of control by the practitioners. Typically, stopping the injection quickly is exceedingly difficult, resulting in an increased risk for leakage. To the best of our knowledge, there are no high-pressure injectors capable of characterizing injection parameters such as injected volume, pressure, and cement flow rate have been reported, even though it was found that observation of these parameters can reduce the risk for cement leakage [24, 25]. Finally, the issue of practitioner exposure to radiation is not satisfactorily addressed with either push-plunger or screw-plunger syringes, because physicians are forced to expose their hands to radiation caused by intraoperative imaging systems such as C-arm-type image intensifiers [26–28].

In light of these circumstances, the authors developed a smart assistive cement injection device. The injection speed and amount of bone cement can be automatically controlled by the host controller. Through the powered motor, pressure pump, hydraulic valve and sterile container, the air inside the bone cement injector was emptied to overcome the influence of air on the injection accuracy, which can improve the accuracy of the injection amount of bone cement, avoiding cement leakage into the spinal canal. It also incorporates immediate flow stop and pressure-limiting mechanisms. What's more, the bone cement injector was installed only once without replacement during the surgical procedure. In addition, the device couples high-pressure cement delivery with parameter control and provides remote activation, reducing the X-ray intake of the surgeon and effectively shortening the duration of the entire operation.

PMMA was obtained by mixing two components: a polymeric powder and a monomeric liquid. The powder incorporates an initiator to encourage polymerization at room temperature and a radiopacifier to render the cement visible on fluoroscopic imaging. The mixing process ends when a homogeneous blend is obtained; the powder is then fully dissolved in the liquid, and the bone cement is relatively liquid. Results of our study indicated that the distribution of bone cement tended to be diffuse or block type in the motorized injection group. In the manual injection group, the distribution of bone cement tended to be a double- or single-band. Postoperative axial CT indicated that the bone cement was distributed more evenly throughout the vertebral body in the motorized than in the manual injection group. A recent study by Li

et al. [29] also proposed that the diffuse and block groups could better maintain vertebral body height and reduce the risk for vertebral body recompression.

Regarding the assessment of X-ray protection, we found that both the fluoroscopy and cement times in the manual injection group were significantly greater than those in the motorized injection group. Previous studies have demonstrated that technical aspects, such as exposure time, distance between the radiation source and patient, and location of the radiation source, influence occupational radiation exposure of surgeons [11]. Theocharopoulos et al. [30] concluded that 90% of an orthopaedic surgeon's effective dose and risk are attributed to kyphoplasty and vertebroplasty. Amar et al. [31] assumed decreased radiation exposure of the surgeon's hand by using a cement delivery system that was remote from the radiograph beam. The present smart assistive bone-cement injection system provides new techniques with lower radiation doses and shorter exposure times to decrease the total radiation dose and achieve maximum possible radiation protection.

The present study had several limitations, the first of which was its use of cadavers—a necessary step, given the current regulatory environment in China. Second, the sample size was limited due to the cost and availability of cadaveric specimens that fulfilled all study criteria. Third, we did not create an injury model that mimicked naturally occurring OVCF. Specific fracture types of future studies will be investigated. Nevertheless, this should not affect the assessment of the feasibility and safety of the assisted bone cement injection system. Despite these challenges and limitations, the potential benefits of a smart-assisted bone cement system in enhancing patient outcomes underscore the need for continued research and development in this field. Future investigations should focus on resolving existing limitations and improving the incorporation of smart systems into surgical workflows.

Conclusions

This study evaluated a system dedicated to bone-cement injection of PVA. The system exhibited more precise control of the bone cement injection dosage and better cement distribution compared with traditional manual injection. In addition, the device provided remote activation, reducing the X-ray intake of the surgeon. Although our results yielded encouraging evidence supporting the feasibility and safety of assisted bone cement injection, additional clinical studies are necessary to corroborate these results and further investigate the potential advantages and drawbacks of this novel technology in clinical practice.

Abbreviations

OVCF	Osteoporotic vertebral compression fracture
PMMA	Poly (methyl methacrylate)
CT	Computed tomography
BL	Body length
BW	Body width
BH	Body height

Acknowledgements

This work was supported by the Medical and Industrial cross research Foundation of "Star of Jiaotong University" Program of Shanghai Jiao Tong University, China (Grant No. YG2022ZD030), the National Natural Science Foundation of China (Grant No. 82401609), the Science and Technology Commission of Shanghai Municipality (Grant No. 24ZR1463700), the Scientific Research Staring Foundation of Shanghai Tongren Hospital (Grant No. TR2023rc10) and Laboratory Open Fund of Key Technology and Materials in Minimally Invasive Spine Surgery of Shanghai Tongren Hospital (Grant No. 2024JZWC-YBB02).

Author contributions

Conceptualization: Chen Jin, Hao-jie Chen, Jiang-ming Yu; Methodology: Chen Jin, Ming-liang Ning; Formal analysis and investigation: Hao-jie Chen; Writing-original draft preparation: Chen Jin; Writing-review and editing: Rui-jun Xu, Xiao-jian Ye; Funding acquisition: Chen Jin, Jiang-ming Yu; Supervision: Jiang-ming Yu.

Funding

This work was supported by the Medical and Industrial cross research Foundation of "Star of Jiaotong University" Program of Shanghai Jiao Tong University, China (Grant No. YG2022ZD030), the National Natural Science Foundation of China (Grant No. 82401609), the Science and Technology Commission of Shanghai Municipality (Grant No. 24ZR1463700), the Scientific Research Staring Foundation of Shanghai Tongren Hospital (Grant No. TR2023rc10) and Laboratory Open Fund of Key Technology and Materials in Minimally Invasive Spine Surgery of Shanghai Tongren Hospital (Grant No. 2024JZWC-YBB02).

Data availability

No datasets were generated or analysed during the current study.

Declarations

Ethics approval and consent to participate

Our research study followed the guidelines and regulations established by the ethics committee of Tongren Hospital, Shanghai Jiao Tong University School of Medicine. The ethics committee of Tongren Hospital, Shanghai Jiao Tong University School of Medicine granted approval for data collection and the conduct of the current cadaveric study.

Consent for publication

Not applicable.

Competing interests

The authors declare no competing interests.

Author details

¹Department of Orthopedics, Tongren Hospital, Shanghai Jiao Tong University School of Medicine, 1111 Xianxia Road, Changning District, Shanghai 200050, China

²Center for Spinal Minimally Invasive Research, Shanghai Jiao Tong University, Shanghai 200050, China

³Department of Orthopedics, Changzhou Geriatric hospital affiliated to Soochow University, Changzhou 213000, China

Received: 23 January 2025 / Accepted: 4 March 2025

Published online: 13 March 2025

References

1. Kendler DL, Bauer DC, Davison KS et al. Vertebral fractures: clinical importance and management. *Am J Med.* 2016;129(2):221.e1-10. <https://doi.org/10.1016/j.amjmed.2015.09.020>
2. Alimy AR, Anastasilakis AD, Carey JJ, et al. Conservative treatments in the management of acute painful vertebral compression fractures: a systematic review and network meta-analysis. *JAMA Netw Open.* 2024;7(9):e2432041. <https://doi.org/10.1001/jamanetworkopen.2024.32041>
3. Huang CC, Hung CC, Chen HM et al. Real world clinical outcomes when discontinuing denosumab or bisphosphonates in patients with surgically managed osteoporotic vertebral compression fractures: a population-based cohort study. *Spine J.* 2024;S1529-9430(24)00942-2. <https://doi.org/10.1016/j.spinee.2024.08.020>
4. Fritzell P, Ohlin A, Borgström F. Cost-effectiveness of balloon kyphoplasty versus standard medical treatment in patients with osteoporotic vertebral compression fracture: a Swedish multicenter randomized controlled trial with 2-year follow-up. *Spine (Phila Pa 1976).* 2011;36(26):2243–51. <https://doi.org/10.1097/BRS.0b013e3182322d0f>
5. Lee JK, Jeong HW, Joo IH, Ko YI, Kang CN. Percutaneous balloon kyphoplasty for the treatment of very severe osteoporotic vertebral compression fractures: a case-control study. *Spine J.* 2018;18(6):962–9. <https://doi.org/10.1016/j.spinee.2017.10.006>
6. McKiernan F, Faciszewski T, Jensen R. Quality of life following vertebroplasty. *J Bone Joint Surg Am.* 2004;86(12):2600–6. <https://doi.org/10.2106/00004623-200412000-00003>
7. Zhu RS, Kan SL, Ning GZ, et al. Which is the best treatment of osteoporotic vertebral compression fractures: balloon kyphoplasty, percutaneous vertebroplasty, or non-surgical treatment? A bayesian network meta-analysis. *Osteoporos Int.* 2019;30(2):287–98. <https://doi.org/10.1007/s00198-018-4804-2>
8. Firanescu CE, de Vries J, Lodder P, et al. Vertebroplasty versus Sham procedure for painful acute osteoporotic vertebral compression fractures (VERTOS IV): randomised Sham controlled clinical trial. *BMJ.* 2018;361:k1551. <https://doi.org/10.1136/bmj.k1551>
9. Eck JC, Nachtigall D, Humphreys SC, Hodges SD. Comparison of vertebroplasty and balloon kyphoplasty for treatment of vertebral compression fractures: a meta-analysis of the literature. *Spine J.* 2008;8(3):488–97. <https://doi.org/10.1016/j.spinee.2007.04.004>
10. Yoo KY, Jeong SW, Yoon W, Lee J. Acute respiratory distress syndrome associated with pulmonary cement embolism following percutaneous vertebroplasty with polymethylmethacrylate. *Spine (Phila Pa 1976).* 2004;29(14):E294–7. <https://doi.org/10.1097/01.brs.0000131211.87594.b0>
11. Harstall R, Heini PF, Mini RL, Orler R. Radiation exposure to the surgeon during fluoroscopically assisted percutaneous vertebroplasty: a prospective study. *Spine (Phila Pa 1976).* 2005;30(16):1893–8. <https://doi.org/10.1097/01.brs.0001174121.48306.16>
12. Loeffel M, Heini PF, Bouduban N, et al. Development of a computer-assisted high-pressure injection device for vertebroplasty. *IEEE Trans Biomed Eng.* 2007;54(11):2051–6. <https://doi.org/10.1109/TBME.2007.894964>
13. Robertson SC. Percutaneous vertebral augmentation: stabilitit a new delivery system for vertebral fractures. *Acta Neurochir Suppl.* 2011;108:191–5. https://doi.org/10.1007/978-3-211-99370-5_29
14. Hu B, Zhang X, Yang Q, et al. Comparison of the efficacy and safety of vertebroplasty with different pedicle approaches for osteoporotic vertebral. *Eur Spine J.* 2024;33(8):3191–212. <https://doi.org/10.1007/s00586-024-08240-7>
15. Chen X, Wang Y, Sheng B, Jiang H. Application of comfortable therapy in percutaneous kyphoplasty (PKP) for osteoporotic vertebral compression fractures. *Asian J Surg.* 2024;47(10):4501–2. <https://doi.org/10.1016/j.asjsur.2024.07.222>
16. Karmakar A, Acharya S, Biswas D, Sau A. Evaluation of percutaneous vertebroplasty for management of symptomatic osteoporotic compression fracture. *J Clin Diagn Res.* 2017;11(8):RC07–10. <https://doi.org/10.7860/JCDR/2017/25886.10461>
17. Xie L, Zhao ZG, Zhang SJ, Hu YB. Percutaneous vertebroplasty versus Conservative treatment for osteoporotic vertebral compression fractures: an updated meta-analysis of prospective randomized controlled trials. *Int J Surg.* 2017;47:25–32. <https://doi.org/10.1016/j.ijsu.2017.09.021>
18. Sun HB, Jing XS, Shan JL, et al. Risk factors for pulmonary cement embolism associated with percutaneous vertebral augmentation: A systematic review and meta-analysis. *Int J Surg.* 2022;101:106632. <https://doi.org/10.1016/j.ijsu.2022.106632>

19. Yang JS, Liu JJ, Chu L, et al. Causes of residual back pain at early stage after percutaneous vertebroplasty: a retrospective analysis of 1,316 cases. *Pain Physician*. 2019;22(5):E495–503.
20. DePuy. Synthes. Vertebroplasty Devices, 2020. Available: <https://www.depuysynthes.com/hcp/spine/products?fq=Vertebroplasty>
21. Stryker. Precision Cement Delivery System, 2020. Available: <https://www.stryker.com/us/en/portfolios/medical-surgical-equipment/image-guided-therapies/vertebral-compression-fractures.html>
22. OptiMed, Cemento-MP. 2020. Available: <https://www.optimed.com/nc/en/products/category/spine/p-kategorie/spine/>
23. Stabilit® vertebral augmentation system, Merit Med. 2021. Available: <https://www.merit.com/merit-interventional/vertebralcompression-fracture/>
24. Phillips FM. Minimally invasive treatments of osteoporotic vertebral compression fractures. *Spine (Phila Pa 1976)*. 2003;28(15 Suppl):S45–53. <https://doi.org/10.1097/01.BRS.0000076898.37566.32>
25. Bohner M, Gasser B, Baroud G, Heini P. Theoretical and experimental model to describe the injection of a polymethylmethacrylate cement into a porous structure. *Biomaterials*. 2003;24(16):2721–30. [https://doi.org/10.1016/s0142-9612\(03\)00086-3](https://doi.org/10.1016/s0142-9612(03)00086-3)
26. Kallmes DF, Roy OE. Radiation dose to the operator during vertebroplasty: prospective comparison of the use of 1-cc syringes versus an injection device. *AJNR Am J Neuroradiol*. 2003;24(6):1257–60.
27. Seibert JA. Vertebroplasty and kyphoplasty: do fluoroscopy operators know about radiation dose, and should they want to know? *Radiology*. 2004;232(3):633–4. <https://doi.org/10.1148/radiol.2323040968>
28. Kouyoumdjian P, Gras-Combe G, Grelat M, et al. Surgeon's and patient's radiation exposure during percutaneous thoraco-lumbar pedicle screw fixation: a prospective multicenter study of 100 cases. *Orthop Traumatol Surg Res*. 2018;104(5):597–602. <https://doi.org/10.1016/j.otsr.2018.05.009>
29. Li KC, Hsieh CH, Liao TH, Cheng BH. A novel classification of cement distribution patterns based on plain radiographs associated with cement filling rate and relevance to the clinical results of unipedicle vertebroplasty. *Eur Spine J*. 2023;32(1):101–9. <https://doi.org/10.1007/s00586-022-07412-7>
30. Theocharopoulos N, Perisinakis K, Damilakis J, et al. Occupational exposure from common fluoroscopic projections used in orthopaedic surgery. *J Bone Joint Surg Am*. 2003;85(9):1698–703. <https://doi.org/10.2106/00004623-2003-09000-00007>
31. Amar AP, Larsen DW, Teitelbaum GP. Use of a screw-syringe injector for cement delivery during kyphoplasty: technical report. *Neurosurgery*. 2003;53(2):380-2; discussion 383. <https://doi.org/10.1227/01.neu.0000073423.09308.40>

Publisher's note

Springer Nature remains neutral with regard to jurisdictional claims in published maps and institutional affiliations.